Korean J. Chem. Eng., 34(7), 2011-2018 (2017)
DOI: 10.1007/s11814-017-0089-y

pISSN: 0256-1115
eISSN: 1975-7220

Isobaric vapor-liquid equilibrium of 2-propanone+2-butanol system at 101.325 kPa: Experimental and molecular dynamics simulation

Hardjono*, Asalil Mustain*,†, Profiyanti Hermien Suharti*, Dhoni Hartanto, and Ianatul Khoiroh*****

*Department of Chemical Engineering, Politeknik Negeri Malang, Jl. Soekarno Hatta No. 9, Malang 65141, Indonesia
**Department of Chemical Engineering, Faculty of Engineering, Universitas Negeri Semarang, Kampus Sekaran, Gunungpati, Semarang 50229, Indonesia
***Department of Chemical and Environmental Engineering, Faculty of Engineering, University of Nottingham Malaysia Campus, Jalan Broga, Semenyih, 43500 Selangor Darul Ehsan, Malaysia
(*Received 1 December 2016 • accepted 26 March 2017*)

Abstract−Isobaric vapor-liquid equilibrium (VLE) data for binary mixtures of 2-propanone+2-butanol have been measured at 101.325 kPa. The measurements were in a modified recirculating type of Othmer equilibrium still. All the data passed the thermodynamics consistency test and no azeotropic behavior was exhibited. The experimental VLE data were correlated with the Wilson, non-random two-liquid (NRTL) and universal quasi-chemical (UNIQUAC) activity coefficient models. The correlation results showed that the experimental data were well correlated with those models. The experimental data also showed slight deviations from the predicted results using UNIFAC and modified UNIFAC (Dortmund) models. To gain more insight into the nature of interactions between 2-propanone molecule and alcohol, we analyzed the hydrogen-bonds, the electrostatic (Coulomb) interactions, and the van der Waals (Lennard-Jones) interaction energies extracted from MD simulations. In addition, the structural property of liquid phase was characterized through radial distribution function (RDF) to establish favorable interactions between 2-propanone and 2-butanol in the mixture.

Keywords: Vapor-liquid Equilibrium, Molecular Dynamic, Ebulliometer, 2-Propanone, 2-Butanol

INTRODUCTION

The production of bioethanol is important since it can be used as a promising substitute for fossil fuel. Therefore, the improvement of bioethanol production has increasingly attracted attention in order to develop a high-efficiency process [1-3]. Bioethanol can be produced via fermentation from sugars by using microorganisms [4-7]. In this process, the fermented product also contains a series of minor compounds, such as other alcohols, carbonyl compounds (2-propanone), organic acids (acetic acid, propionic acid) and esters (methyl acetate, ethyl acetate) [8]. Those multicomponent mixtures need to be separated to achieve high purity of bioethanol. The most commonly used method in the purification process is distillation. Thermodynamic knowledge, vapor-liquid equilibrium (VLE), is therefore needed in the design and improvement of a distillation column [9-11]. In the case of bioethanol purification, VLE data for each pair of components among the fermented product mixtures should be generated.

The isobaric binary VLE data for the components encountered in the alcohol separation process have been compiled in the previous study [12,13]. To the best of our knowledge, the VLE data for binary mixture of 2-propanone+2-butanol measured at 101.325 kPa are not available in the open literature. For this reason, the binary VLE data for the above-mentioned system have been determined in this study. These data were measured by using a modified recirculating type of Othmer equilibrium still. The Herington method [14] was employed to verify the thermodynamic consistency of the experimental data. The results obtained were further correlated with the Wilson [15], nonrandom two-liquid (NRTL) [16] and universal quasichemical (UNIQUAC) [17] models. The experimental data were also compared with the predictive UNIFAC [18] and modified UNIFAC (Dortmund) [19] models as well. To investigate the favorable interactions between 2-propanone and 2-butanol in the mixture, intermolecular energies and hydrogen bond were analyzed. Finally, the structural property of liquid phase was also characterized through radial distribution function (RDF).

EXPERIMENTAL SECTION

1. Materials

Analytical grade 2-propanone and 2-butanol supplied from commercial sources were used in this work. The mass fraction purity level of 2-propanone and 2-butanol are better than 0.9975 and 0.9900, respectively. 2-propanone was purchased from Mallinckrodt (Ireland) and 2-butanol was from Merck (Germany). All materials were used as received. The details of each compounds used in this work are reported in Table 1.

2. Apparatus and Experimental Procedures

The isobaric VLE data were determined by using a modified Othmer-type recirculating still. The operation procedure of apparatus

†To whom correspondence should be addressed.
E-mail: asalil89@polinema.ac.id, asalil89@yahoo.com

Table 1. Properties of pure components

Component	Supplier	Mass fraction purity	MW ($g \cdot mol^{-1}$)	Purification method
2-Propanone	Mallinckrodt (Ireland)	0.9975	58.080	None
2-Butanol	Merck (Germany)	0.9900	74.123	None

is described in detail by Hartanto et al. [20]. A mixture containing 2-propanone and 2-butanol at specific compositions was prepared and charged into an ebulliometer. The total volume of the solution used in the measurement was about 150 cm^3 for each experimental run. A heater equipped with a magnetic stirrer was used to provide proper heating and mixing for the loaded solution.

The pressure adjustment system equipped with a water reservoir as an elevation-control and a graduated burrete connected to the still was used to maintain the pressure in the ebulliometer to be constant at (101.325±0.200) kPa since the local atmospheric pressure was below 101.325 kPa. A barometer (Germany) with an accuracy of ±0.1 kPa was used to measure the local atmospheric pressure. The water level difference in the water reservoir and a graduate burette were adjusted to complement the pressure difference between local atmospheric pressure and standard atmospheric pressure of 101.325 kPa.

The equilibrium condition in the ebulliometer was assumed to be achieved when steady temperature and pressure were obtained for at least 60 min or longer. Then, the equilibrium temperature was recorded. The equilibrium temperature was measured by a calibrated digital thermometer type-K (TK4S-14RN, USA) with an accuracy of ±0.1 K. The condensed vapour samples and liquid samples were taken for gas chromatograph (GC) analysis.

3. Sample Analysis

The condensed vapor samples and liquid samples were injected by syringe into a gas chromatograph. The composition of collected sample was further analyzed by a gas chromatograph (Hewlett Packard Model 5890, USA) equipped with a flame ionization detector (FID) and a stainless-steel column with Carbowax 30M. High purity nitrogen (>0.999 in mass fraction) was used as a carrier gas with a constant flowrate of 28 $cm^3 \cdot min^{-1}$. The temperature condition of the GC was set at 372.15 K for injector, 318.15 K for oven and 448.15 K for the detector, respectively. The GC response for each sample was calculated using a TotalChrom Navigator system. Calibration curves were constructed for the investigated system to convert the area fraction of each sample obtained from GC into the mole fraction. Several compositions of standard solution were prepared gravimetrically by using an analytical balance (Shinova Model FA2204B, China) with an accuracy of ±0.0001 g for the whole composition range.

4. Molecular Dynamics Simulation

2-Propanone and 2-butanol were all described using the OPLS-AA force field [21]. The OPLS-AA topology and structure file for 2-propanone was taken from the Virtual Chemistry database [22]. Density functional theory (DFT) calculations were performed in Gaussian 09 [23] to calculate the atomic charges for this alcohol. The Becke gradient corrected exchange and Lee-Yang-Parr correlation functional with the three parameters (B3LYP) method with the 6-311G were selected as a basis set [24].

All simulations for pure components and binary system were at 298.15 K by using GROMACS package version 4.6.4 [25]. An environment with a concentration of 0.2500, 0.5000, and 0.7500 mole fraction of 2-propanone was modelled by mixing a total of 1000 molecules in the mixture. For the simulation box, a cubic box type with periodic boundary conditions applied in three directions of the Cartesian coordinates was selected. Energy minimizations were performed for 5×10^5 steps using the steepest-descent method to ensure the removal of all kinetic energy in the system. Since the starting configuration was most likely very far from equilibrium; to ensure the equilibrium of all the properties within the system, a preliminary series of simulations was conducted. The systems were stirred in an *NVT* (constant number of particles, constant volume, and constant temperature) ensemble at 298.15 K for 1 ns. Finally, production simulations were carried out in the isothermal and isobaric *NPT* (constant number of particles, constant pressure, and constant temperature) ensemble at 298.15 K and 1 bar for 5 ns. For each system, the first 4 ns were discarded and only the last 1 ns was used for analysis. The Newton equation was solved using the leap-frog stochastic dynamic integrator with time step of 2 fs. For the short range electrostatic (Coulomb) interactions, a twin-range 0.9 nm cut-off was used; for the Lennard-Jones (van der Waals) interaction 1.4 nm was used. For every ten simulation steps at this distance, the neighbor searching was updated. Long range electrostatic interactions were evaluated using smooth particle mesh Ewald (PME) method [26] with a cubic interpolation and maximum grid spacing of 0.125 nm. The reference temperature was controlled by chained Nose-Hoover thermostat [27] with time constant for coupling of 1.0 ps. The Parrinello-Rahman [28] pressure coupling barostat was used with the relaxation time of 2.0 ps. The bonds in the molecules were constrained using the linear constraint solver (LINCS) algorithm [29] with a fourth-order in the expansion of the constraint coupling matrix. The simulated trajectories were saved and written every 0.2 ps in the disk. In every configuration, stable potential energy was the criterion for equilibration. The block averaging method was applied to calculate the errors in the calculated densities.

RESULTS AND DISCUSSION

1. Experimental Vapor-liquid Equilibrium

The experimental VLE data for binary systems of 2-propanone+ 2-butanol were measured at 101.325 kPa using a modified recirculating type of Othmer equilibrium still. The experimental data measured in this work are presented in Table 2. The measured boiling point of pure 2-propanone and 2-butanol in Table 2 was also compared with the literature data to validate our measurement method. The comparison results show that those measured boiling points were in good agreement with the literature data as the deviations in boiling point were less than 0.2 K. The graphical presentation of the data measurements is given in Fig. 1. As can be seen, azeotropic behavior was not observed for the investigated binary system.

Table 2. Vapor-liquid equilibrium data for binary system of 2-propanone (1)+2-butanol (2) at 101.325 kPa[a]

T (K)	x_1	y_1
372.8; 372.9[b]; 372.7[c]	0.0000	0.0000
370.0	0.0238	0.1817
365.1	0.0662	0.3940
357.0	0.2153	0.6217
354.2	0.2789	0.6756
351.4	0.3280	0.7173
345.2	0.4698	0.8314
343.2	0.5301	0.8572
342.0	0.5767	0.8839
339.2	0.6280	0.9218
337.3	0.6973	0.9379
335.0	0.8172	0.9628
329.4; 329.5[d]; 329.3[e]	1.0000	1.0000

[a]u(T)=0.1 K, u(P)=0.100 kPa, u(x_1)=0.0010 and u(y_1)=0.0010
[b]Ref. [32] [c]Ref. [33] [d]Ref. [34] [e]Ref. [35]

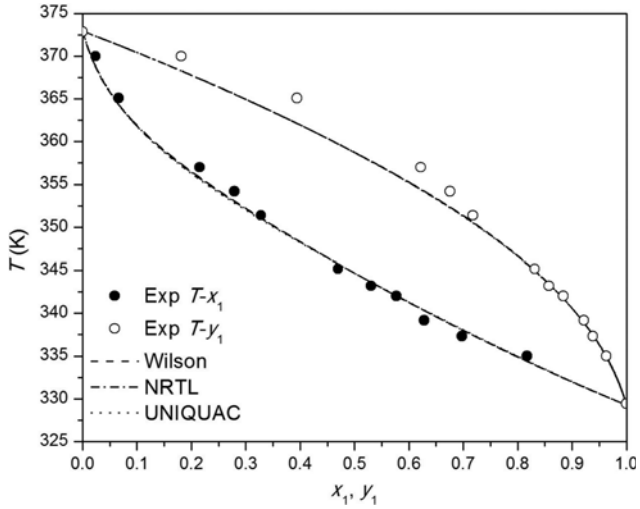

Fig. 1. VLE phase (T-x_1-y_1) diagram for binary system of 2-propanone (1)+2-butanol (2) at 101.325 kPa.

The experimental data were then tested using thermodynamic consistency test with Herington test method to confirm the reliability of the data measurements [14]. The experimental data are considered thermodynamically consistent if the values of |D−J|<10. D and J are defined below:

$$D = 100\left|\frac{A-B}{A+B}\right| \tag{1}$$

$$J = 150\left|\frac{T_{max}-T_{min}}{T_{min}}\right| \tag{2}$$

where A is the area above the zero line on the diagram of $\ln(\gamma_1/\gamma_2)$ vs x_1; and B is the area under the zero line on this diagram. T_{max} and T_{min} are the highest and the lowest boiling temperature, respectively. The value of |D−J| for 2-propanone+2-butanol system was 9.78. The results showed that all the experimental data passed the consistency test criterion.

Table 3. Parameters of the extended Antoine equation[a] for pure compounds

Component	A	B	C	D	E
2-Propanone	62.0982	−5599.6	−7.0985	6.224×10^{-6}	2
2-Butanol	115.642	−10236	−14.125	2.356×10^{-17}	6

[a]P_i^s is in kPa and T is in K

Table 4. Physical properties and parameters of pure components used in the activity coefficients correlation

No.	Component	r[a]	q[a]
1	2-Propanone	2.5735	2.336
2	2-Butanol	3.5979	3.032

[a]Determined from the Bondi method [36]

In the VLE data reduction, the vapor phase was assumed as ideal gas because the measured condition in this study was at low pressure (101.325 kPa) and the liquid phase was considered as non-ideal mixtures. The following equation can be used to describe the VLE relationship for those conditions:

$$y_i P = x_i \gamma_i P_i^s \tag{3}$$

where x_i is the liquid phase mole fractions of component i and y_i is the vapor phase mol fractions of component i. γ_i is the activity coefficients of component i. P is the system pressure and P_i^s is the vapor pressures of the pure component i, which is calculated by the extended Antoine equation:

$$\ln(P_i^s) = A + \frac{B}{T} + C\ln T + DT^E \tag{4}$$

The constants of extended Antoine equation, A, B, C, D and E, used in this work are in Table 3.

The measured experimental VLE data (T-x_1-y_1) were further correlated with the Wilson, NRTL and UNIQUAC activity coefficient models to determine the binary interaction parameters for the binary mixtures of 2-propanone (1)+2-butanol (2). For UNIQUAC model, the area parameter (q) and volume parameter (r) of pure components used in the correlation are given in Table 4. The maximum likelihood principle [30] was chosen to determine the optimal binary interaction parameters of that mixture by minimizing the objective function (OF) as shown below:

$$OF = \sum_{k=1}^{n_p}\left\{\left[\frac{(P_k^{cal}-P_k^{exp})}{\sigma_P}\right]^2 + \left[\frac{(T_k^{cal}-T_k^{exp})}{\sigma_T}\right]^2 + \left[\frac{(x_{1,k}^{cal}-x_{1,k}^{exp})}{\sigma_{x_1}}\right]^2 + \left[\frac{(y_{1,k}^{cal}-y_{1,k}^{exp})}{\sigma_{y_1}}\right]^2\right\} \tag{5}$$

where n_p is the number of data points. The superscripts of "cal" and "exp" denote the calculated and the experimental values, respectively. The standard deviations of pressure, temperature, liquid phase mole fraction of component 1 and vapor phase mole fraction of component 1 are 0.2 kPa, 0.1 K, 0.005 and 0.005, respectively.

The correlation results are listed in Table 5, which consists of

Table 5. Fitted binary interaction parameters of activity coefficient models for binary system of 2-propanone (1)+2-butanol (2)

Model	Parameters				RMSD[a]			
	A_{12}	A_{21}	B_{12} (K)	B_{21} (K)	ΔT (K)	ΔP (kPa)	Δx_1	Δy_1
Wilson[b]	−12.5484	1.3246	4036.52	−286.29	0.70	0.221	0.0006	0.0251
NRTL[c]	−4.7041	17.2600	1375.72	−5576.80	0.72	0.226	0.0007	0.0246
UNIQUAC[d]	2.6147	−8.3133	−733.24	2615.58	0.76	0.235	0.0007	0.0244

[a] RMSD $\Delta M = \left(\frac{1}{n_p} \sum_{k=1}^{n_p} (M_k^{cal} - M_k^{exp})^2 \right)^{0.5}$

where n_p is the number of data points and M represents T, P, x_1 or y_1

[b] $\tau_{ij} = \exp\left(A_{ij} + \frac{B_{ij}}{T}\right)$

[c] $\tau_{ij} = A_{ij} + \frac{B_{ij}}{T}$, the value of α is fixed to be 0.3

[d] $\tau_{ij} = \exp\left(A_{ij} + \frac{B_{ij}}{T}\right)$

Table 6. Group specifications for each component

Component	Main group	Sub group	No.	$v_k^{(i)}$	R_k	Q_k
UNIFAC [37]						
2-Propanone	1	CH_3	1	1	0.9011	0.848
	9	CH_3CO	19	1	1.6724	1.488
2-Butanol	1	CH_3	1	2	0.9011	0.848
	1	CH_2	2	1	0.6744	0.540
	1	CH	3	1	0.4469	0.228
	5	OH	15	1	1.0000	1.200
Modified UNIFAC (Dortmund) [38]						
2-Propanone	1	CH_3	1	1	0.6325	1.0608
	9	CH_3CO	18	1	1.7048	1.6700
2-Butanol	1	CH_3	1	2	0.6325	1.0608
	1	CH_2	2	1	0.6325	0.7081
	1	CH	3	1	0.6325	0.3554
	5	OH (s)	81	1	1.0630	0.8663

the best fitted binary interaction parameters and the root mean square deviations (RMSD) between the experimental results and the calculated values. The results show that the experimental VLE data were well correlated with the Wilson, NRTL and UNIQUAC models. The experimental data and the calculated values with those models are also compared graphically in Fig. 1.

Table 7. UNIFAC group-group interaction parameters, a_{mn}, in K [37]

Main group	n=1	5	9
m=1	0	986.5	476.4
5	156.4	0	84.00
9	26.76	164.5	0

In addition, the experimental VLE data were also compared with the predictive activity coefficient models such as UNIFAC and modified UNIFAC (Dortmund). The volume and surface area parameters, R_k and Q_k, of those models for each component are listed in Table 6. While, the interaction parameters between the existing UNIFAC and modified UNIFAC (Dortmund) main groups are presented in Tables 7 and 8, respectively. The interaction parameters between the same main groups are set equal to zero in both models. The comparison results between the experimental data with the prediction values are compiled in Table 9 and illustrated graphically in Fig. 2. Based on the RMSD and AARE values and graphical illustration, the modified UNIFAC (Dortmund) model gave better prediction than that of the UNIFAC model since the main group alcohol (OH) was separated into primary, secondary and tertiary alcohol group in the modified UNIFAC (Dortmund).

2. Structural Properties of Binary Mixture from MD Simulation

The reliability of the force field is validated by comparing cer-

Table 8. Modified UNIFAC (Dortmund) group-group interaction parameters [38]

m	n	a_{mn} (K)	b_{mn}	c_{mn} (K^{-1})	a_{nm} (K)	b_{nm}	c_{nm} (K^{-1})
1	1	0.0	0.0	0.0	0.0	0.0	0.0
1	5	2777.0	−4.6740	0.1551×10^{-2}	1606.0	−4.7460	0.9181×10^{-3}
1	9	433.60	0.1473	0.0	199.00	−0.8709	0.0
5	5	0.0	0.0	0.0	0.0	0.0	0.0
5	9	−250.0	2.8570	-0.6022×10^{-2}	653.30	−1.4120	0.9540×10^{-3}
9	9	0.0	0.0	0.0	0.0	0.0	0.0

Table 9. The RMSD and AARE in boiling points (ΔT) and vapor-phase mole fraction (Δy_1) from predicted results using the UNIFAC and modified UNIFAC (Dortmund) with the experimental data

Model	RMSD[a]		AARE[b]	
	ΔT (K)	Δy_1	ΔT (%)	Δy_1 (%)
UNIFAC	2.77	0.0355	0.64	5.74
Modified UNIFAC (Dortmund)	1.86	0.0433	0.46	6.85

[a]RMSD $\Delta M = \left(\frac{1}{n_p} \sum_{k=1}^{n_p} (M_k^{cal} - M_k^{exp})^2 \right)^{0.5}$

[b]AARE $\Delta M = \frac{1}{n_p} \sum_{k=1}^{n_p} \left| \frac{M_k^{cal} - M_k^{exp}}{M_k^{exp}} \right| \cdot 100\%$

where n_p is the number of data points and M represents T or y_1

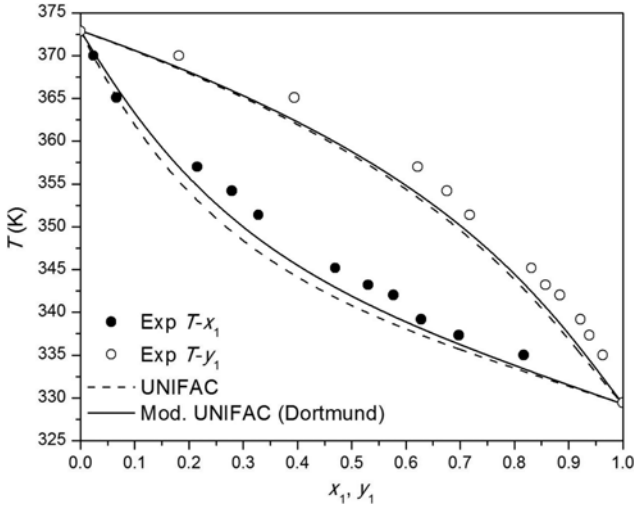

Fig. 2. Comparison the experimental VLE data of 2-propanone (1)+2-butanol (2) at 101.325 kPa with the predictive models.

tain properties from experiment and computational results. In this study, densities of pure component and binary mixture with x_1= 0.5000 at 298.15 K and atmospheric pressure were calculated and compared to the values available in the reference. As can be seen from Table 10, good agreement was found between simulated and experimental densities. Thus, it can be assumed that all simulations of binary mixtures are reliable for analysis of other properties. Fig. 3 shows snapshots obtained from MD simulations for the studies system.

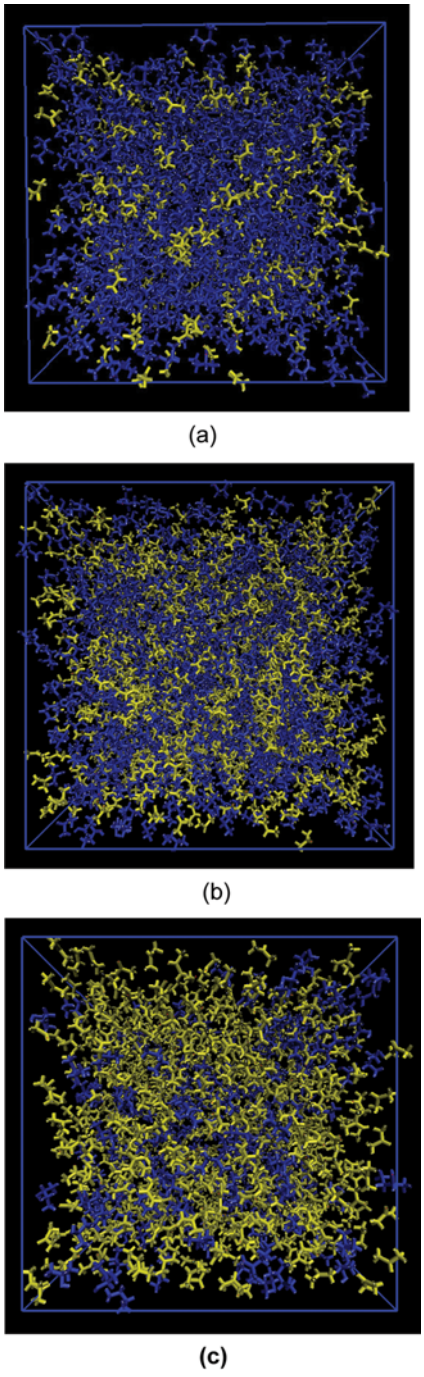

Fig. 3. Snapshot for the configuration of the 2-propanone (yellow) and 2-butanol (blue) after 6 ns simulation for (a) x_1=0.25; (b) x_1=0.5; (c) x_1=0.75.

Table 10. Simulated and experimental densities for solvents and binary systems at 298.15 K

System	ρ_{exp} (kg·m^{-3})	ρ_{exp} (kg.m^{-3})	Error[a] (%)
2-Propanone	787.03	784.29 [39]; 778.68 [40]	0.35; 1.07
2-Butanol	788.04	802.60 [39]; 798.25 [40]	1.81; 1.28
2-Propanone+2-butanol (x_1=0.500)	779.04	790.30 [39]	1.42

[a]Error $\Delta\rho = \left| \frac{\rho_k^{sim} - \rho_k^{exp}}{\rho_k^{exp}} \right| \cdot 100\%$

Table 11. The average number of hydrogen bonds, the electrostatic (Coulomb) and the van-der Waals (Lennard-Jones) energies obtained from the MD simulations for the interaction of 2-propanone and 2-butanol

x_1	H-bonds per 2-propanone	Couloumb ($kJ \cdot mol^{-1}$)	Lennard-Jones ($kJ \cdot mol^{-1}$)
0.25	0.162	−57182.1	6243.65
0.50	0.228	−112654.0	8536.56
0.75	0.006	−55891.2	2290.67

The formation of H-bonds of the binary mixture was observed by quantitative analysis of average number of intramolecular hydrogen bonds formed by alcohol molecules at different concentration. This result is tabulated in Table 11. The average number of hydrogen bonds per molecule was determined from the trajectories based on a geometrical criterion with a cutoff donor-acceptor (DA) distance of at most 0.35 nm and a cutoff donor-hydrogen-acceptor (DHA) angle of at most 30°. OH groups are regarded as donors and O as an acceptor. It is apparent that the average number of hydrogen bonds per 2-propanone with alcohol molecule is less than one per molecule for all the concentration studied. Briefly, the number of H-bonds observed for 2-propanone and 2-butanol system was 0.162 (x_1=0.250), 0.228 (x_1=0.50), and 0.006 (x_1=0.750), respectively. The analysis of the nature of the interaction energies between 2-propanone molecules with 2-butanol is further strengthened in Table 11. The intermolecular energy considered in the calculation is only the hetero (2-propanone-alcohol) contribution, both for electrostatic (Coulomb) and the van-der Waals (Lennard-Jones) energy terms. Intermolecular energies for this mixture were found to be dominated by the Coulomb for more than 90% to those of Lennard-Jones contribution for all composition analyzed. Since it is generally accepted that H-bonds are predominantly electrostatic interactions in origin [21], we can conclude that the most significant interaction between 2-propanone in 2-butanol is clearly due to the Coulomb interaction.

Although the interaction energy based on H-bond formation for binary mixtures of 2-propanone with 2-butanol is very low and found to be insignificant compared with the van der Waals contribution, it is still interesting to analyze the distribution of the solvents around the oligomer and the interactions relevant to H-bonds formation through radial distribution functions (RDFs). RDFs are typically used to describe the structure of liquids. They give the probability of finding a particle at the distance r, from another particle and therefore provide a quantitative description of enhancement or depletion of densities of atoms, or groups of atoms, around a selected moiety with respect to bulk values. Real RDFs can be acquired experimentally through neutron or X-ray scattering. The establishment of a hydrogen bond is one of the most important features that can be highlighted for the binary system studied. The presence of hydrogen bonds is recognizable by the presence of a site-to-site RDF Y-H-X with a distance smaller than 0.26 nm, where Y is an oxygen or nitrogen atom and X an oxygen atom. Additionally, weaker H-bonds can be observed from a site-to-site RDF with the first minimum in a distance smaller than 0.40 nm, where Y is an oxygen or nitrogen atom and X a carbon atom. In the studied systems, the first minimum found was 0.26 and 0.35 nm for anion-solvent and solvent-solvent interactions, and cation-solvent and cation-anion interactions, respectively.

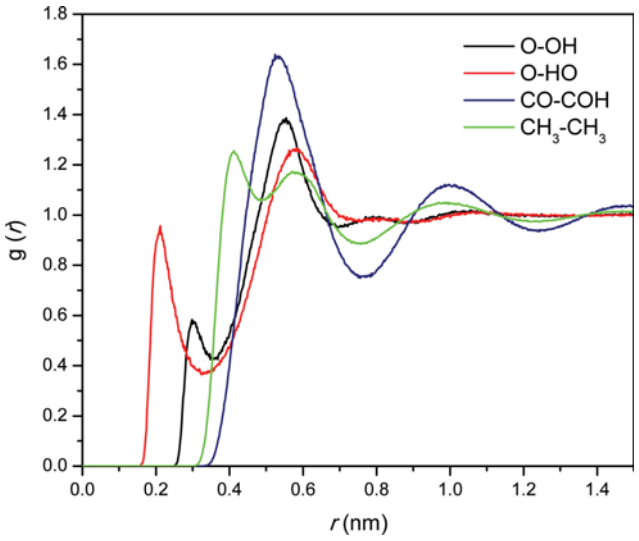

Fig. 4. RDFs of the O-OH, O-HO, CO-COH, and CH_3-CH_3 interaction for binary system of 2-propanone (1)+2-butanol at x_1= 0.2500.

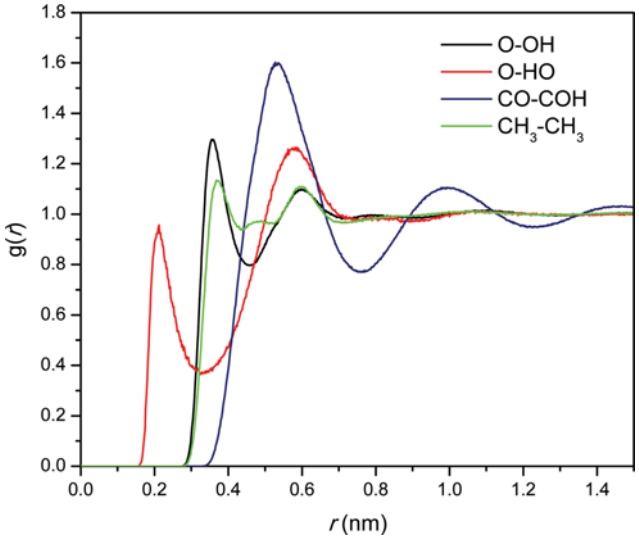

Fig. 5. RDFs of the O-OH, O-HO, CO-COH, and CH_3-CH_3 interaction for binary system of 2-propanone (1)+2-butanol at x_1= 0.5000.

The analysis of solvent-solvent interactions for a binary mixture of 2-propanone and 2-butanol are depicted in Figs. 4-6. These RDFs provide the analysis based on the site-to-site RDFs for four different pairs, namely O-OH, O-HO, CO-COH, and CH_3-CH_3, at x_1=0.2500, 0.5000, and 0.7500, respectively. O refers to the oxygen atom of 2-propanone, where OH and HO stand for protons and oxygen atoms in 2-butanol molecule. CO is the carbon atoms of 2-propanone and COH is the central carbon atom of alcohol. While, CH_3 is the alkyl carbon atom for 2-propanone and 2-butanol. From Figs. 4 and 5, the appearance of the first peak which

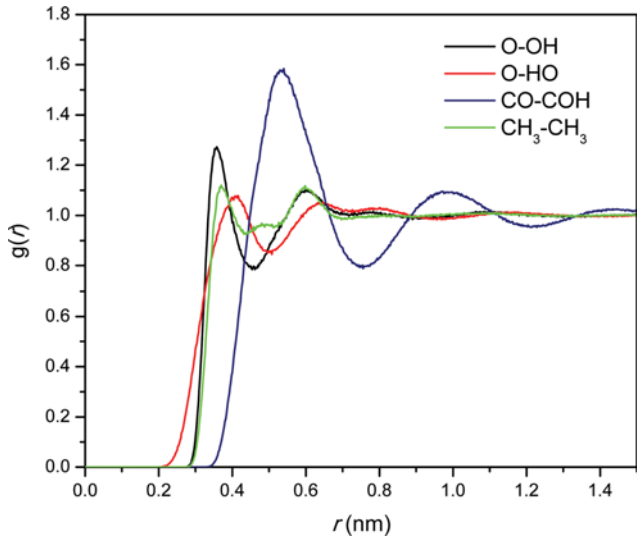

Fig. 6. RDFs of the O-OH, O-HO, CO-COH, and CH_3-CH_3 interaction for binary system of 2-propanone (1)+2-butanol at x_1= 0.7500.

categorized as H-bond formation, occured at distance of 0.216 nm for 2-propanone composition of 0.25 and 0.212 nm for x_1=0.5000. Weaker hydrogen bond formation is observed for higher concentration of 2-propanone, i.e., x_1=0.7500, as depicted in Fig. 6 where the first minimum is observed at a distance of 0.40 nm. Additionally, each peak of CO-COH and CH_3-CH_3 interactions is almost located in the same position. The first peak of CO-COH for all composition appears at 0.54 nm and the first peak of CH_3-CH_3 interaction is pronounced at 0.412 nm, respectively. Thus, we can conclude that the first peak of CH_3-CH_3 interaction presents somehow stronger intermolecular interaction due to the higher density region. Note that 2-propanone-alcohol interactions also show a double peak of RDF, suggesting the non-ideality behavior observed for the binary system studied [31].

CONCLUSION

Isobaric VLE data for binary system of 2-propanone+2-butanol have been determined. The apparatus used was a modified recirculating type of Othmer equilibrium still. The experimental data passed the thermodynamic consistency test using the Herington test method. No azeotropic behavior was exhibited in the observed system. The experimental data were well correlated with the Wilson, NRTL and UNIQUAC models because the deviations between experimental data and calculated values were relatively low. For the comparison results with the predictive models, the modified UNIFAC (Dortmund) model could give better VLE prediction compared to UNIFAC model. Finally, MD simulations were performed for binary mixture studied at three different compositions. The nature of the interaction energies between 2-propanone and alcohol was determined by computing the average number of hydrogen bonds and by analyzing the intermolecular interaction energies. We concluded that the most significant contribution is due to electrostatic effect. The MD trajectories were used to calculate radial distributions, which were used to infer the nature and profile of the interaction established between 2-propanone and 2-butanol.

ACKNOWLEDGEMENTS

This research was supported by Penelitian Dana DIPA Politeknik Negeri Malang under Contract No: 6123/PL2.1/HK/2016. The authors also would like to thank C. Sarasati and F.D. Cahyani for their support in the VLE measurement.

SUPPORTING INFORMATION

Additional information as noted in the text. This information is available via the Internet at http://www.springer.com/chemistry/journal/11814.

REFERENCES

1. B. Klinpratoom, A. Ontanee and C. Ruangviriyachai, *Korean J. Chem. Eng.*, **32**, 413 (2015).
2. S. Khan, M. Ul-Islam, W. A. Khattak, M. W. Ullah, B. Yu and J. K. Park, *Korean J. Chem. Eng.*, **32**, 694 (2015).
3. M. Han, Y. Kim, W.-S. Cho, G.-W. Choi and B.-W. Chung, *Korean J. Chem. Eng.*, **33**, 223 (2016).
4. A. K. Chandel, R. K. Kapoor, A. Singh and R. C. Kuhad, *Bioresour. Technol.*, **98**, 1947 (2007).
5. K. Karimi, G. Emtiazi and M. J. Taherzadeh, *Process Biochem.*, **41**, 653 (2006).
6. C. Martín, M. Galbe, C. F. Wahlbom, B. Hahn-Hägerdal and L. J. Jönsson, *Enzyme Microb. Technol.*, **31**, 274 (2002).
7. M. Han, Y. Kim, Y. Kim, B. Chung and G.-W. Choi, *Korean J. Chem. Eng.*, **28**, 119 (2011).
8. T. P. V. B. Dias, L. A. A. P. Fonseca, M. C. Ruiz, F. R. M. Batista, E. A. C. Batista and A. J. A. Meirelles, *J. Chem. Eng. Data*, **59**, 659 (2014).
9. G. Wibawa, A. Mustain, M. F. Akbarina and R. M. Ruslim, *J. Chem. Eng. Data*, **60**, 955 (2015).
10. A. Wiguno, A. Mustain, W. F. E. Irwansyah and G. Wibawa, *Indones. J. Chem.*, **16**, 111 (2016).
11. W. J. Jeong, H.-k. Cho and J. S. Lim, *Korean J. Chem. Eng.*, **33**, 2961 (2016).
12. A. Mustain, D. Hartanto and S. Altway, *ARPN J. Eng. Appl. Sci.*, **11**, 3465 (2016).
13. A. Mustain, A. Takwanto and D. Hartanto, *Jurnal Bahan Alam Terbarukan*, **5**, 37 (2016).
14. E. F. G. Herington, *J. Inst. Pet.*, **37**, 457 (1951).
15. G. M. Wilson, *J. Am. Chem. Soc.*, **86**, 127 (1964).
16. H. Renon and J. M. Prausnitz, *AIChE J.*, **14**, 135 (1968).
17. D. S. Abrams and J. M. Prausnitz, *AIChE J.*, **21**, 116 (1975).
18. A. Fredenslund, R. L. Jones and J. M. Prausnitz, *AIChE J.*, **21**, 1086 (1975).
19. U. Weidlich and J. Gmehling, *Ind. Eng. Chem. Res.*, **26**, 1372 (1987).
20. D. Hartanto, B. S. Gupta, M. Taha and M.-J. Lee, *J. Chem. Thermodyn.*, **98**, 159 (2016).
21. W. L. Jorgensen, D. S. Maxwell and J. Tirado-Rives, *J. Am. Chem. Soc.*, **118**, 11225 (1996).

22. D. van der Spoel, P. J. van Maaren and C. Caleman, *Bioinformatics*, **28**, 752 (2012).
23. M. J. Frisch, G. W. Trucks, H. B. Schlegel, P. M. W. Gill, B. G. Johnson, M. A. Robb, J. R. Cheeseman, T. A. Keith, G. A. Petersson, J. A. Montgomery Jr., K. Raghavachari, M. A. Al-Laham, V. G. Zakrzewski, J. V. Ortiz, J. B. Foresman, C. Y. Peng, P. A. Ayala, M. W. Wong, J. L. Andres, E. S. Replogle, R. Gomperts, R. L. Martin, D. J. Fox, J. S. Binkley, D. J. Defrees, J. Baker, J. P. Stewart, M. Head-Gordon, C. Gonzalez and J. A. Pople, *Gaussian 94, Revision A.1*, Gaussian, Inc., Pittsburgh, PA (1995).
24. A. D. Becke, *J. Chem. Phys.*, **98**, 5648 (1993).
25. E. Lindahl, B. Hess and D. van der Spoel, *Molecular Modeling Annual*, **7**, 306 (2001).
26. T. Darden, D. York and L. Pedersen, *J. Chem. Phys.*, **98**, 10089 (1993).
27. S. Nosé, *Mol. Phys.*, **52**, 255 (1984).
28. M. Parrinello and A. Rahman, *J. Appl. Phys.*, **52**, 7182 (1981).
29. B. Hess, *J. Chem. Theory Comput.*, **4**, 116 (2008).
30. T. F. Anderson, D. S. Abrams and E. A. Grens, *AIChE J.*, **24**, 20 (1978).
31. I. Khan, M. L. S. Batista, P. J. Carvalho, L. M. N. B. F. Santos, J. R. B. Gomes and J. A. P. Coutinho, *J. Phys. Chem. B*, **119**, 10287 (2015).
32. J. Wisniak and A. Tamir, *J. Chem. Eng. Data*, **20**, 388 (1975).
33. K. J. Miller and H.-S. Huang, *J. Chem. Eng. Data*, **17**, 77 (1972).
34. N. Gultekin, *J. Chem. Eng. Data*, **34**, 168 (1989).
35. H.-C. Ku and C.-H. Tu, *Fluid Phase Equilib.*, **231**, 99 (2005).
36. A. Bondi, *Physical Properties of Molecular Crystals, Liquids and Glasses*, Wiley, New York (1968).
37. H. K. Hansen, P. Rasmussen, A. Fredenslund, M. Schiller and J. Gmehling, *Ind. Eng. Chem. Res.*, **30**, 2352 (1991).
38. J. Gmehling, J. Li and M. Schiller, *Ind. Eng. Chem. Res.*, **32**, 178 (1993).
39. B. Orge, M. Iglesias, G. Marino and J. Tojo, *J. Chem. Thermodyn.*, **31**, 497 (1999).
40. K. R. Patil, G. Pathak and S. D. Pradhan, *Thermochim. Acta*, **177**, 143 (1991).

Supporting Information

Isobaric vapor-liquid equilibrium of 2-propanone+2-butanol system at 101.325 kPa: Experimental and molecular dynamics simulation

Hardjono*, Asalil Mustain*,†, Profiyanti Hermien Suharti*, Dhoni Hartanto, and Ianatul Khoiroh*****

*Department of Chemical Engineering, Politeknik Negeri Malang, Jl. Soekarno Hatta No. 9, Malang 65141, Indonesia
**Department of Chemical Engineering, Faculty of Engineering, Universitas Negeri Semarang,
Kampus Sekaran, Gunungpati, Semarang 50229, Indonesia
***Department of Chemical and Environmental Engineering, Faculty of Engineering,
University of Nottingham Malaysia Campus, Jalan Broga, Semenyih, 43500 Selangor Darul Ehsan, Malaysia
(*Received 1 December 2016 • accepted 26 March 2017*)

Table S1. Topology file for acetone and the calculated atomic charges. Molecular structure and its atomic numbering is given in Fig. S1.

```
[ moleculetype ]
; Name            nrexcl
acetone           3

[ atoms ]
;   nr       type  resnr residue  atom   cgnr     charge       mass
     1   opls_280      1     ACE     C      1       0.47     12.011
     2   opls_135      1     ACE     C      2      −0.18     12.011
     3   opls_135      1     ACE     C      3      −0.18     12.011
     4   opls_281      1     ACE     O      4      −0.47    15.9994
     5   opls_282      1     ACE     H      5       0.06      1.008
     6   opls_282      1     ACE     H      6       0.06      1.008
     7   opls_282      1     ACE     H      7       0.06      1.008
     8   opls_282      1     ACE     H      8       0.06      1.008
     9   opls_282      1     ACE     H      9       0.06      1.008
    10   opls_282      1     ACE     H     10       0.06      1.008

[ bonds ]
1       2       1       0.153     265265.6
1       3       1       0.152     265265.6
1       4       1       0.122     476976.0
2       6       1       0.109     284512.0
2       5       1       0.109     284512.0
2       7       1       0.108     284512.0
3       9       1       0.109     284512.0
3       8       1       0.109     284512.0
3       10      1       0.109     284512.0

[ angles ]
1       2       6       1       110.948     292.880
1       2       5       1       109.346     292.880
1       2       7       1       111.833     292.880
1       3       9       1       108.033     292.880
1       3       8       1       120.736     292.880
1       3       10      1       105.470     292.880
```

2	1	3	1	116.722	585.760
2	1	4	1	119.852	669.440
3	1	4	1	119.505	669.440
5	2	6	1	107.047	276.144
5	2	7	1	109.185	276.144
6	2	7	1	108.350	276.144
8	3	9	1	106.564	276.144
8	3	10	1	103.806	276.144
9	3	10	1	112.271	276.144

[dihedrals]

3 1 2 6 3	0.57530	1.72590	0.00000	−2.30120	0.00000	0.00000
4 1 2 6 3	0.00000	0.00000	0.00000	0.00000	0.00000	0.00000
3 1 2 5 3	0.57530	1.72590	0.00000	−2.30120	0.00000	0.00000
4 1 2 5 3	0.00000	0.00000	0.00000	0.00000	0.00000	0.00000
3 1 2 7 3	0.57530	1.72590	0.00000	−2.30120	0.00000	0.00000
4 1 2 7 3	0.00000	0.00000	0.00000	0.00000	0.00000	0.00000
2 1 3 9 3	0.57530	1.72590	0.00000	−2.30120	0.00000	0.00000
4 1 3 9 3	0.00000	0.00000	0.00000	0.00000	0.00000	0.00000
2 1 3 8 3	0.57530	1.72590	0.00000	−2.30120	0.00000	0.00000
4 1 3 8 3	0.00000	0.00000	0.00000	0.00000	0.00000	0.00000
2 1 3 10 3	0.57530	1.72590	0.00000	−2.30120	0.00000	0.00000
4 1 3 10 3	0.00000	0.00000	0.00000	0.00000	0.00000	0.00000

[dihedrals]

2 3 1 4 1	improper_O_C_X_Y	180.0	43.93200	2

[pairs]

6	3	1
6	4	1
5	3	1
5	4	1
7	3	1
7	4	1
9	2	1
9	4	1
8	2	1
8	4	1
10	2	1
10	4	1

Table S2. Topology file for 2-butanol and the calculated atomic charges. Molecular structure and its atomic numbering is given in Fig. S2.

[moleculetype]

; Name	nrexcl
2-butanol	3

[atoms]

; nr	type	resnr	residue	atom	cgnr	charge	mass
1	opls_136	1	LIG	C1	1	−0.317	12.011
2	opls_135	1	LIG	C2	4	−0.544	12.011
3	opls_135	1	LIG	C3	8	−0.494	12.011
4	opls_158	1	LIG	C4	12	−0.035	12.011
5	opls_154	1	LIG	O1	14	−0.593	15.9994

6	opls_140	1	LIG	H1	2	−0.179	1.008
7	opls_155	1	LIG	H2	15	−0.357	1.008
8	opls_140	1	LIG	H3	9	−0.187	1.008
9	opls_140	1	LIG	H4	10	−0.184	1.008
10	opls_140	1	LIG	H5	11	−0.165	1.008
11	opls_140	1	LIG	H6	5	−0.185	1.008
12	opls_140	1	LIG	H7	6	−0.165	1.008
13	opls_140	1	LIG	H8	7	−0.172	1.008
14	opls_140	1	LIG	H9	3	−0.167	1.008
15	opls_140	1	LIG	H10	13	−0.153	1.008

[bonds]

1	2	1	0.152	224262.4
1	4	1	0.151	224262.4
1	6	1	0.111	284512.0
1	14	1	0.111	284512.0
2	11	1	0.111	284512.0
2	12	1	0.111	284512.0
2	13	1	0.111	284512.0
3	4	1	0.151	224262.4
3	8	1	0.111	284512.0
3	9	1	0.111	284512.0
3	10	1	0.111	284512.0
4	5	1	0.140	267776.0
4	15	1	0.111	284512.0
5	7	1	0.094	462750.4

[angles]

1	2	11	1	110.011	313.800
1	2	12	1	110.046	313.800
1	2	13	1	110.046	313.800
1	4	3	1	109.498	488.273
1	4	5	1	107.685	418.400
1	4	15	1	109.376	313.800
2	1	4	1	109.498	488.273
2	1	6	1	109.389	313.800
2	1	14	1	109.389	313.800
3	4	5	1	107.727	418.400
3	4	15	1	109.421	313.800
4	1	6	1	109.425	313.800
4	1	14	1	109.425	313.800
4	3	8	1	109.967	313.800
4	3	9	1	110.046	313.800
4	3	10	1	110.046	313.800
4	5	7	1	106.910	460.240
5	4	15	1	113.068	292.880
6	1	14	1	109.702	276.144
8	3	9	1	108.977	276.144
8	3	10	1	108.977	276.144
9	3	10	1	108.799	276.144
11	2	12	1	108.954	276.144
11	2	13	1	108.954	276.144
12	2	13	1	108.799	276.144

[dihedrals]

4 1 2 11	3	0.62760	1.88280	0.00000	−2.51040	0.00000	0.00000
6 1 2 11	3	0.62760	1.88280	0.00000	−2.51040	0.00000	0.00000
14 1 2 11	3	0.62760	1.88280	0.00000	−2.51040	0.00000	0.00000
4 1 2 12	3	0.62760	1.88280	0.00000	−2.51040	0.00000	0.00000
6 1 2 12	3	0.62760	1.88280	0.00000	−2.51040	0.00000	0.00000
14 1 2 12	3	0.62760	1.88280	0.00000	−2.51040	0.00000	0.00000
4 1 2 13	3	0.62760	1.88280	0.00000	−2.51040	0.00000	0.00000
6 1 2 13	3	0.62760	1.88280	0.00000	−2.51040	0.00000	0.00000
14 1 2 13	3	0.62760	1.88280	0.00000	−2.51040	0.00000	0.00000
2 1 4 3	3	2.92880	−1.46440	0.20920	−1.67360	0.00000	0.00000
6 1 4 3	3	0.62760	1.88280	0.00000	−2.51040	0.00000	0.00000
14 1 4 3	3	0.62760	1.88280	0.00000	−2.51040	0.00000	0.00000
2 1 4 5	3	2.87441	0.58158	2.09200	−5.54799	0.00000	0.00000
6 1 4 5	3	0.97905	2.93716	0.00000	−3.91622	0.00000	0.00000
14 1 4 5	3	0.97905	2.93716	0.00000	−3.91622	0.00000	0.00000
2 1 4 15	3	0.62760	1.88280	0.00000	−2.51040	0.00000	0.00000
6 1 4 15	3	0.62760	1.88280	0.00000	−2.51040	0.00000	0.00000
14 1 4 15	3	0.62760	1.88280	0.00000	−2.51040	0.00000	0.00000
8 3 4 1	3	0.62760	1.88280	0.00000	−2.51040	0.00000	0.00000
9 3 4 1	3	0.62760	1.88280	0.00000	−2.51040	0.00000	0.00000
10 3 4 1	3	0.62760	1.88280	0.00000	−2.51040	0.00000	0.00000
8 3 4 5	3	0.97905	2.93716	0.00000	−3.91622	0.00000	0.00000
9 3 4 5	3	0.97905	2.93716	0.00000	−3.91622	0.00000	0.00000
10 3 4 5	3	0.97905	2.93716	0.00000	−3.91622	0.00000	0.00000
8 3 4 15	3	0.62760	1.88280	0.00000	−2.51040	0.00000	0.00000
9 3 4 15	3	0.62760	1.88280	0.00000	−2.51040	0.00000	0.00000
10 3 4 15	3	0.62760	1.88280	0.00000	−2.51040	0.00000	0.00000
1 4 5 7	3	−0.44350	3.83255	0.72801	−4.11705	0.00000	0.00000
3 4 5 7	3	−0.44350	3.83255	0.72801	−4.11705	0.00000	0.00000
15 4 5 7	3	0.94140	2.82420	0.00000	−3.76560	0.00000	0.00000

[pairs]

11	4	1
11	6	1
11	14	1
12	4	1
12	6	1
12	14	1
13	4	1
13	6	1
13	14	1
3	2	1
3	6	1
3	14	1
5	2	1
5	6	1
5	14	1
15	2	1
15	6	1
15	14	1
1	8	1
1	9	1
1	10	1
5	8	1
5	9	1
5	10	1

15	8	1
15	9	1
15	10	1
7	1	1
7	3	1
7	15	1

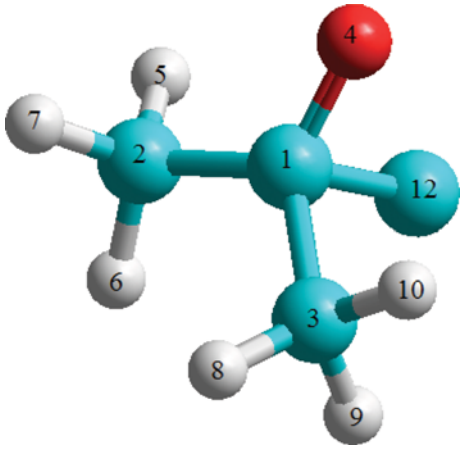

Fig. S1. Acetone molecule with its atomic numbering. The hydrogen atoms were depicted by white colour, carbon atoms by blue, and oxygen atoms by red.

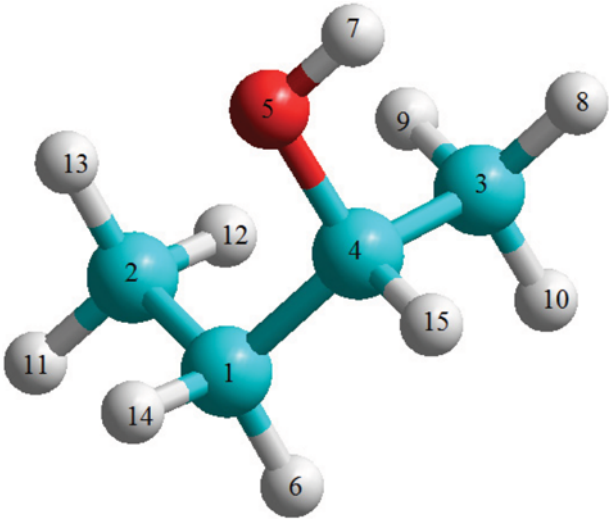

Fig. S2. 2-Butanol molecule with its atomic numbering. The hydrogen atoms were depicted by white colour, carbon atoms by blue, and oxygen atoms by red.